Kinematic wave model for transient bed profiles in alluvial channels under nonequilibrium conditions

Gokmen Tayfur[1] and Vijay P. Singh[2]

Received 31 October 2006; revised 22 May 2007; accepted 19 July 2007; published 27 December 2007.

[1] Transient bed profiles in alluvial channels are generally modeled using diffusion (or dynamic) waves and assuming equilibrium between detachment and deposition rates. Equilibrium sediment transport can be considerably affected by an excess (or deficiency) of sediment supply due to mostly flows during flash floods or floods resulting from dam break or dike failure. In such situations the sediment transport process occurs under nonequilibrium conditions, and extensive changes in alluvial river morphology can take place over a relatively short period of time. Therefore the study and prediction of these changes are important for sustainable development and use of river water. This study hence developed a mathematical model based on the kinematic wave theory to model transient bed profiles in alluvial channels under nonequilibrium conditions. The kinematic wave theory employs a functional relation between sediment transport rate and concentration, the shear-stress approach for flow transport capacity, and a relation between flow velocity and depth. The model satisfactorily simulated transient bed forms observed in laboratory experiments.

Citation: Tayfur, G., and V. P. Singh (2007), Kinematic wave model for transient bed profiles in alluvial channels under nonequilibrium conditions, *Water Resour. Res.*, *43*, W12412, doi:10.1029/2006WR005681.

1. Introduction

[2] Generally alluvial river processes evolve over a long period of time. However, some extreme events like a flash flood or flood resulting from dam break or a dike failure may cause extensive changes in alluvial river morphology over a relatively short period of time, in the order of few hours [*Singh et al.*, 2004]. In such a situation, the transport involves the processes of both the aggradation (deposition) due to excess sediment supply and degradation (entrainment) due to deficiency in sediment supply. In general, these processes of aggradation and degradation take place under nonequilibrium conditions. The study and prediction of changes in river morphology is important for sustainable development and use of river water [*Singh et al.*, 2004].

[3] Aggradation and degradation processes in alluvial rivers have been extensively experimentally and mathematically investigated. Experimental studies involved mostly laboratory flume experiments since they provide controlled replication of particular combinations of initial and boundary conditions [*Curran and Wilcock*, 2005]. Among many experimental studies, *Soni* [1981a] studied aggradation process under equilibrium conditions. *Yen et al.* [1992] investigated aggradation and degradation processes in a steady flow conditions. *Wilcock et al.* [2001] studied mixture of sand and gravel transport by carrying out 48 sets of experiments of flow, transport, and bed grain size using five different sediments in a laboratory flume. *Tang and Knight* [2006] carried out laboratory sediment transport experiments in which they investigated the effect of floodplain roughness on bed form geometry, bed load transport, and dune migration rate. Experimental studies enhanced our understanding of basic mechanisms of the sediment transport processes and enabled us to develop mathematical models that can emulate and thus study the behavior of the dynamics.

[4] There have been many mathematical models for studying aggradation and degradation processes in alluvial channels. *Lyn and Altinakar* [2002] developed solution to the St.Venant-Exner equations as a model for bed evolution under conditions when the Froude number approaches unity and quasi-steady model becomes singular. *Wilcock and Crowe* [2003] and *Curran and Wilcock* [2005] developed models for investigating effect of sand supply on the transport rate of gravel bed rivers. They used constant flow rate, flow depth and gravel feed rate but varied the sand supply. *Singh et al.* [2004] investigated modeling of bed profiles under a dike failure. *Li and Millar* [2007] modified two-dimensional hydrodynamic bed model to simulate bed load transport in a complex gravel bed river. They tested their model against field data.

[5] Mathematical models developed for sediment transport and evolution of transient bed profiles in alluvial rivers are generally based on either diffusion wave [*de Vries*, 1973; *Soni*, 1981b, 1981c; *Ribberink and Van Der Sande*, 1985; *Lisle et al.*, 2001] or dynamic wave [*Ching and Cheng*, 1964; *Vreugdenhil and de Vries*, 1973; *de Vries*, 1975; *Ribberink and Van Der Sande*, 1985; *Pianese*, 1994; *Lyn and Altinakar*, 2002; *Cao and Carling*, 2003; *Singh et al.*, 2004; *Mohammadian et al.*, 2004; *Li and Millar*, 2007]. In both representations, the sediment transport function is

[1]Department of Civil Engineering, Izmir Institute of Technology, Izmir, Turkey.
[2]Department of Biological and Agricultural Engineering, Texas A&M University, College Station, Texas, USA.

0043-1397/07/2006WR005681$09.00

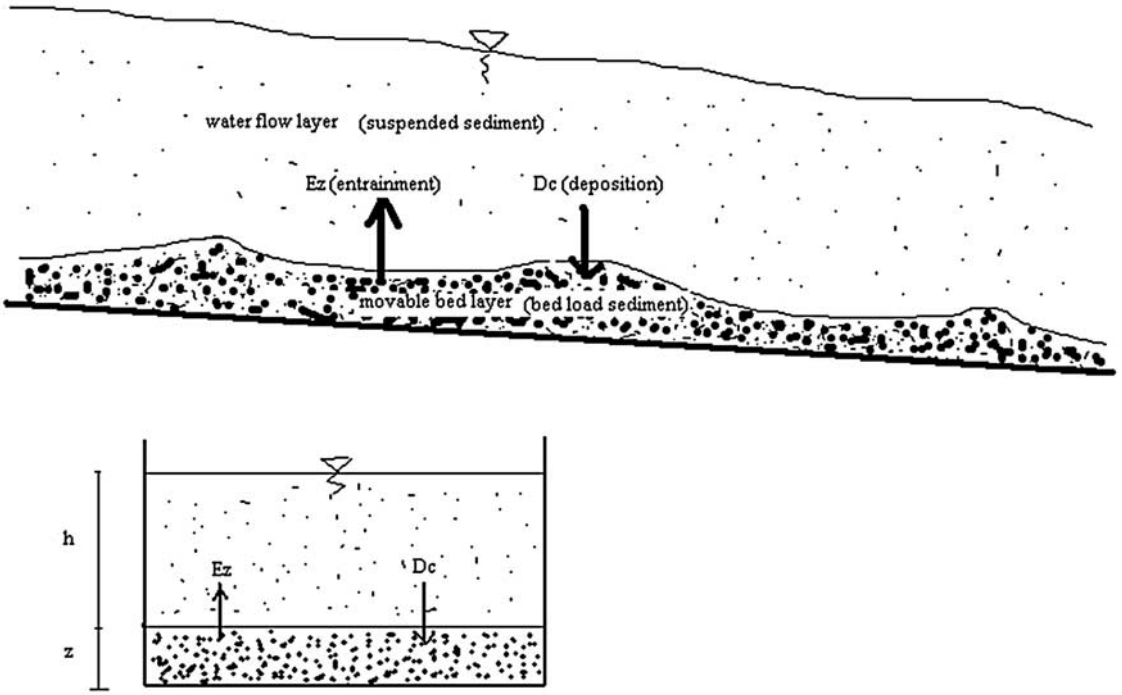

Figure 1. Schematic representation of two-layer system.

mostly represented as a functional relation between sediment flux and water flow variables. The experimental studies by *Langbein and Leopold* [1968] on bead movement in a flume; sand movement in pipes; sand movement in flumes, and gravel and cobble movement in Santa Fe River, however, revealed that there is a strong relation between sediment transport rate and sediment concentration. They provided evidence that the evolution and movement of bed profiles could be treated as a kinematic wave, with a functional relation between sediment transport rate and concentration. This was further shown by *Tayfur and Singh* [2006], who modeled transient bed profiles under equilibrium transport conditions using kinematic wave theory. They tested their model against laboratory data obtained under equilibrium transport conditions in a steady uniform flow.

[6] Like *Tayfur and Singh* [2006], most of the studies in the literature have assumed equilibrium conditions between detachment rate and deposition rate. In other words, they have assumed that there is no interchange of sediment particles between suspended load and bed load such that these two loads are in equilibrium. This may be true for the cases where flow and sediment discharges, channel geometry, and water and sediment properties remain constant for a long period of time. However, it is highly likely that these variables would change owing to flash floods or floods due to dam break or dike failure or human activities within the river reach. Flash floods may cause heavy erosion and landslides in a river basin causing sediment overloading within a river reach. Flood wave due to dam break may cause underloading owing to its excessive flow transport capacity. Human activities within a river section may cause overloading or underloading. Overloading causes aggradation, while underloading results in degradation in a river bed. During aggradation the river flow capacity is exceeded and consequently suspended sediment deposits on the river bed, whereas during degradation the river flow capacity detaches particles from the bed layer and infuses them into suspension. As such, there may be an exchange of sediment particles between bed layer and suspended layer, depending upon the flow transport capacity of a river and sediment supply, resulting in nonequilibrium conditions for transient bed forms.

[7] The objective of this study is to develop a mathematical model, using the kinematic wave theory, for describing the bed profile evolution and movement in alluvial channels under nonequilibrium conditions, and test the model using measured data. *Tayfur and Singh* [2006], on the basis of kinematic wave theory, developed sediment transport model for simulating transient bed profiles in alluvial channels under equilibrium conditions and tested their model against laboratory experimental data of aggradation. The main contribution of the current study, however, would be the development of transport equations for transient sediment waves in alluvial channels, using the same kinematic wave theory, under nonequilibrium conditions and testing the model against the aggradation and degradation experimental data.

2. Mathematical Model

[8] The bed profile evolution and movement in alluvial channels can be represented, as shown in Figure 1, as a system involving two layers: water flow layer and movable bed layer. The water flow layer may contain suspended sediment. The movable bed layer consists of water and sediment particles and therefore has porosity. There may be an exchange of sediment between the two layers, depending

upon the flow transport capacity and sediment rate in suspension. For a wide rectangular alluvial channel with constant width, the conservation of mass equations for water and sediment, considering both the layers, on a unit width can be written as [*Tayfur and Singh*, 2006]

$$\frac{\partial h(1-c)}{\partial t}+\frac{\partial hu(1-c)}{\partial x}+p\frac{\partial z}{\partial t}=q_{lw}, \tag{1}$$

$$\frac{\partial hc}{\partial t}+\frac{\partial huc}{\partial x}+(1-p)\frac{\partial z}{\partial t}+\frac{\partial q_{bs}}{\partial x}=q_{ls}, \tag{2}$$

where h is the flow depth (L), u is the flow velocity (L/T), c is the volumetric sediment concentration in the water flow phase (in suspension) (L^3/L^3), p is the bed sediment porosity (L^3/L^3), z is the mobile bed layer elevation (L), q_{lw} is the lateral water flux (L/T), q_{bs} is the sediment flux in the movable bed layer (L^2/T), q_{ls} is the lateral sediment flux (L/T), x is the independent variable representing the coordinate in the longitudinal direction (flow direction) (L), and t is the independent variable of time (T).

[9] Equations (1) and (2) are for the conservation of water and sediment in both the layers, respectively. Simpler versions of equations (1) and (2) have been employed in the literature [*Ching and Cheng*, 1964; *Vreugdenhil and de Vries*, 1973; *Mahmood*, 1975; *Pianese*, 1994; *Cao and Carling*, 2003]. Note that equations (1) and (2) are for equilibrium conditions, where the entrainment rate (E_z) is equal to the deposition rate (D_c) (i.e., $E_z = D_c$). In other words, the suspended sediment load and bed load are in equilibrium such that there is no detachment of particles from the movable bed layer and there is no deposition of suspended sediment on the bed layer.

[10] Under nonequilibrium conditions ($E_z \neq D_c$), there is, however, much confusion in the literature in writing the right system of equations. *Pianese* [1994], who employed the dynamic wave approximation for sediment wave, used one equation for the conservation of water (equation (1)) and one for the conservation of sediment (equation (2)) in both the layers (Figure 1). In addition, he employed one more equation called adaptation equation (or lag equation) relating the change in bed level in time to flow variables (u, h), equilibrium suspended sediment concentration (c_{eq}) which is, in turn, expressed as a function of flow variables, and suspended sediment concentration (c) [*Pianese*, 1994] as

$$(1-p)\frac{\partial z}{\partial t}=\frac{uh}{\lambda}\left(c_{eq}-c\right), \tag{3}$$

where λ is called the adaptation length. The right-hand side of equation (3) represents the deposition rate (positive) or detachment rate (negative) [*Pianese*, 1994]. According to equation (3), when there is detachment z is supposed to decrease while c increases. Similarly, when there is deposition z should increase but c has to decrease. If one were to substitute equation (3) into equation (2), $(1-p)\frac{\partial z}{\partial t}$ would disappear from the equation. Most recently, using the dynamic wave approximation for bed profiles, *Mohammadian et al.* [2004] employed one equation for the conservation of water, equation (1) (although they assumed $c = 0$ in equation (1)), and one equation for the conservation of suspended sediment in the water flow layer as

$$\frac{\partial hc}{\partial t}+\frac{\partial huc}{\partial x}=\frac{\partial}{\partial x}\left(V_x h\frac{\partial c}{\partial x}\right)+\frac{v_f}{\eta}\left(c_{eq}-c\right), \tag{4}$$

where V_x is the sediment mixing coefficient, v_f is the sediment particle fall velocity, and η is a coefficient. The last term on the right-hand side of equation (4) represents the deposition rate (negative) or detachment rate (positive). In addition, they employed the following equation for relating the change in bed level in time to the particle fall velocity, equilibrium suspended sediment concentration (c_{eq}), and suspended sediment concentration (c) as

$$(1-p)\frac{\partial z}{\partial t}=\frac{v_f}{\eta}\left(c_{eq}-c\right). \tag{5}$$

Although equations (4) and (5), respectively, seem to be for the conservation of suspended sediment in the water flow layer and sediment in the movable bed layer under nonequilibrium conditions, there seem some deficiencies. The last term on the right-hand side of equation (4) acts as a source, when it is positive ($c_{eq} > c$), for suspended sediment concentration but it, in turn, acts as a sink for concentration in the bed layer. In this case, there should be a negative sign in front of the term on the right-hand side of equation (5). Second, equation (5) does not fully represent the conservation of mass equation for the sediment in the movable bed layer, since it ignores the major term of the sediment flux gradient $\left(\frac{\partial q_{bs}}{\partial x}\right)$. In other words, *Mohammadian et al.* [2004] employed only equations (1), (4), and (5) for modeling the process. In other words, they did not employ equation (2) and therefore consequently ignored the bed sediment flux term.

[11] In order to avoid any confusion, this study proposes to write the conservation of mass for suspended sediment in the water flow layer and conservation of mass for bed sediment in the movable bed layer separately, considering the exchange of sediment due to the detachment and deposition between the two layers. From the point of view of basic physical processes of sediment transport, these equations can simply be written as

$$\frac{\partial hc}{\partial t}+\frac{\partial huc}{\partial x}=q_{lsus}+\frac{1}{\rho_s}[E_z-D_c], \tag{6}$$

$$(1-p)\frac{\partial z}{\partial t}+\frac{\partial q_{bs}}{\partial x}=q_{lbed}+\frac{1}{\rho_s}[D_c-E_z], \tag{7}$$

where q_{lsus} is the lateral suspended sediment (L/T), q_{lbed} is the lateral bed load sediment (L/T), ρ_s is the sediment mass density (M/L^3), E_z is the entrainment rate (detachment rate) ($M/L^2/T$), and D_c is the deposition rate ($M/L^2/T$).

[12] Equations (6) and (7) are for the conservation of mass for the suspended sediment and conservation of sediment in the movable bed layer, respectively. Note that when $E_z \neq D_c$, the process is in the nonequilibrium condition. When $E_z > D_c$, there is entrainment from the bed layer, thus reducing the bed elevation but increasing the suspended sediment concentration. When $E_z < D_c$, there is

deposition, thus increasing the bed level but reducing the suspended sediment concentration. When $E_z = D_c$, there is no exchange of sediment between the two layers and the process is in equilibrium.

[13] Under equilibrium conditions ($E_z = D_c$), equations (6) and (7) are generally combined into a single equation (expressed by equation (2)) for the conservation of sediment in both the layers. Also, under equilibrium conditions, suspended sediment concentration is expressed as a function of flow variables, and equations (1) and (2), together with the momentum equation, are solved to simulate the transient bed profiles [*Ching and Cheng*, 1964; *de Vries*, 1975; *Pianese*, 1994].

[14] Equations (1), (6), and (7) are for the conservation of mass for water in both the layers, suspended sediment in the water flow layer, and sediment in the movable bed layer, respectively, and constitute the basic equations for modeling transient bed profiles under equilibrium ($E_z = D_c$) and nonequilibrium conditions ($E_z \neq D_c$). According to equations (1), (6), and (7), there are five unknowns, namely, h, u, c, z, and q_{bs}. In order to close the system, two more equations are needed. One equation can be obtained using the momentum equation for water flow. This study employed the kinematic wave approximation for the momentum equation:

$$u = \alpha\, h^{\beta-1}, \tag{8}$$

where α is the depth-velocity coefficient ($L^{0.5}/T$) [*Singh*, 1996] and β is an exponent. Employing Chezy's equation for the friction slope, $\beta = 1.5$ and $\alpha = C_z S_f^{0.5}$, where C_z is the Chezy roughness coefficient ($L^{0.5}/T$) and S_f is the friction slope that is taken as equal to the bed slope, S_o.

[15] The fifth equation can be obtained by relating sediment transport rate (sediment flux) to sediment concentration in the movable bed layer. Previous researchers [*de Vries*, 1965; *de Vries*, 1973; *Mahmood*, 1975; *Phillips and Sutherland*, 1983; *Ribberink and Van Der Sande*, 1985; *Hotchkiss and Parker*, 1991; *Cao and Carling*, 2003] have related sediment flux in the movable bed layer to the flow variables in the water flow layer and have used a complete dynamic wave or diffusion waveform of the momentum equation. In this study, the kinematic wave theory was, however, employed. Following *Tayfur and Singh* [2006],

$$q_{bs} = (1-p)v_s z\left[1 - \frac{z}{z_{\max}}\right], \tag{9}$$

where v_s = the velocity of sediment particles as concentration approaches zero (L/T) and $z_{\max}$ is the maximum bed elevation (L).

[16] Equations (8) and (9), together with equations (1), (6), and (7), form the system of five equations for modeling the evolution and movement of bed forms in alluvial channels under nonequilibrium conditions. Combining equations (8) and (9) with equations (1), (6), and (7), the system of equations, after a little algebraic manipulation, can be written in a compact form as

$$\frac{\partial h}{\partial t} + \alpha\beta h^{\beta-1}\frac{\partial h}{\partial x} + \frac{p}{(1-c)}\frac{\partial z}{\partial t} - \frac{h}{(1-c)}\frac{\partial c}{\partial t} - \frac{\alpha h^{\beta}}{(1-c)}\frac{\partial c}{\partial x} = \frac{q_{lw}}{(1-c)}, \tag{10}$$

$$\frac{\partial c}{\partial t} + \alpha h^{\beta-1}\frac{\partial c}{\partial x} + \frac{c}{h}\frac{\partial h}{\partial t} + c\alpha\beta h^{\beta-2}\frac{\partial h}{\partial x} = \frac{q_{lsus}}{h} + \frac{1}{\rho_s h}[E_z - D_c], \tag{11}$$

$$\frac{\partial z}{\partial t} + v_s\left[1 - \frac{2z}{z_{\max}}\right]\frac{\partial z}{\partial x} = \frac{q_{ls}}{(1-p)} + \frac{1}{(1-p)\rho_s}[D_c - E_z]. \tag{12}$$

Equations (10)–(12) represent the kinematic wave equations for modeling non–steady state, nonuniform transient channel bed profiles under nonequilibrium conditions. Note that the same system of equations can model transient bed profiles under equilibrium conditions when $D_c = E_z$. The last term on the right-hand side of equation (11) represents the net detachment rate. It is positive when $E_z > D_c$ and consequently some of sediment are infused upward from the bed layer into the flow layer (degradation process). The last term on the right-hand side of equation (12) represents the net deposition rate. It is positive when $D_c > E_z$, and some sediment particles in the suspension phase move downward settling on the bed layer (aggradation process).

[17] The detachment rate (E_z), using the shear-stress approach, can be expressed as [*Yang*, 1996]

$$E_z = \sigma\, T_c = \sigma\left[\Phi(\tau - \tau_{cr})^k\right], \tag{13}$$

where

$$\tau = \gamma_w h S_o, \tag{14}$$

$$\tau_{cr} = \kappa(\gamma_s - \gamma_w)d_s, \tag{15}$$

where σ is the transfer rate coefficient (1/L), T_c is the flow transport capacity (M/L/T), Φ is the soil erodibility coefficient, τ, is the shear stress (M/L^2), τ_c is the critical shear stress (M/L^2), k is an exponent, γ_w is the specific weight of water (M/L^3), γ_s is the specific weight of sediment (M/L^3), κ is a constant, and d_s is the sediment particle diameter (L). The deposition rate can be expressed as [*Yang*, 1996]

$$D_c = \sigma\rho_s q_{ss} = \sigma[\rho_s huc], \tag{16}$$

where q_{ss} is the unit suspended sediment discharge (M/L/T).

[18] According to equations (10)–(16), the processes of water flow, suspended sediment, and bed sediment transport are interlinked not only throughflow variables (h, u), channel characteristics (C_z, S_o), and sediment characteristics (ρ_s, γ_s, d_s) but also the sediment particle velocity v_s which is a function of particle characteristics and flow variables.

[19] On the basis of theoretical considerations of the dynamics of bed load motion, *Bridge and Dominic* [1984] developed the following expression for grain velocity:

$$v_s = \delta\left(u_* - u_{*c}\right), \tag{17}$$

where δ is defined as

$$\delta = \frac{1}{K} \ln\left(\frac{y_n}{y_1}\right), \tag{18}$$

where K is the von Karman constant, y_n is the distance from the boundary of effective fluid thrust on bed load grain, and y_1 is the roughness height. The average value of δ is between 8 and 12 [*Bridge and Dominic*, 1984]. This study employed a value of $\delta = 10$. Value u_{*c} is the critical shear velocity (shear velocity at the incipient motion) and is defined as [*Bridge and Dominic*, 1984]

$$u_{*c} = \frac{v_f(\tan\phi)^2}{\delta}, \tag{19}$$

where $\tan\phi$ is the dynamic friction coefficient and has an average value between 0.48 and 0.58 [*Bridge and Dominic*, 1984]. This study employed a value of $\tan\phi = 0.53$. As seen in equation (19), the critical shear velocity is a function of particle fall velocity. Analyzing a wide range of empirical data, *Dietrich* [1982] developed the following equation for particle fall velocity [*Dietrich*, 1982; *Bridge and Bennett*, 1992]:

$$W_* = R_3 10^{(R_1+R_2)}, \tag{20}$$

where

$$R_1 = -3.767 + 1.929(\log D_*) - 0.0982(\log D_*)^2 - 0.00575(\log D_*)^3 + 0.00056(\log D_*)^4, \tag{21}$$

$$R_2 = \log\left[1 - \frac{(1-CSF)}{0.85}\right] - (1-CSF)^{2.3}\tanh[\log D_* - 4.6] + 0.3(0.5-CSF)(1-CSF)^2(\log D_* - 4.6), \tag{22}$$

$$R_3 = \left[0.65 - \left(\frac{CSF}{2.83}\tanh[\log D_* - 4.6]\right)\right]^{\left[1+\frac{(3.5-P)}{2.5}\right]}, \tag{23}$$

where the dimensionless settling (fall) velocity of the particle (W_*) is expressed as [*Dietrich*, 1982]

$$W_* = \frac{\rho v_f^3}{(\rho_s - \rho)g\nu}, \tag{24}$$

where ρ is the fluid (water) density. The dimensionless particle size (D_*) is expressed as [*Dietrich*, 1982]

$$D_* = \frac{(\rho_s - \rho)g d_s^3}{\rho\nu^2}. \tag{25}$$

[20] The Corey shape factor (*CSF*) is defined as [*Dietrich*, 1982]

$$CSF = \frac{c}{(ab)^{0.5}}, \tag{26}$$

where a, b, and c are the longest, intermediate, and shortest axes of the sediment, respectively, and are mutually perpendicular. The mean value of *CSF* for most naturally occurring sediment is between 0.5 and 0.8 [*Dietrich*, 1982]. This study employed an average value of $CSF = 0.65$. P is the Powers value of roundness that has an average value between 3.5 and 6 [*Dietrich*, 1982]. This study employed the value of $P = 4.75$. Note that equation (20) considers the influence of grain shape as well as density and size on the fall velocity of a particle.

[21] The model parameters basically are as follows: C_z, p, S_o, $z_{\max}$, ρ_s, γ_s, σ, Φ, ϕ, k, κ, *CSF*, P, and d_s. Parameters ρ_s, γ_s, and d_s can be obtained from experimental sediment data, while S_o, C_z, and p can be obtained from field measurements. *Langbein and Leopold* [1968] suggest $C_{\max} = 245$ kg/m^2 (*note that* $z_{\max} = \frac{C_{\max}}{(1-p)\rho_s}$). *Gessler* [1965] suggested a value of 0.047 for κ for most flow conditions. The value of σ has a wide range of 1.0–30.0 m^{-1}, parameter Φ has a range of 0.0–1.0, and exponent k_i has a range of 1.0–2.5 in the literature [*Foster*, 1982; *Tayfur*, 2002; *Yang*, 1996]. Equations (10)–(12) are solved numerically, subject to the specified initial and boundary conditions. The initial conditions can be specified as

$$h(x,0) = h_o, \tag{27}$$

$$c(x,0) = c_o, \tag{28}$$

$$z(x,0) = z_o, \tag{29}$$

where h_o, c_o, and z_o are the initial flow depth (L), the initial suspended sediment concentration (L^3/L^3), and the initial bed-level elevation (L), respectively. Since the kinematic wave approximation is used for both flow and sediment transport, the model requires only the specification of the upstream boundary conditions. The upstream boundary conditions can be specified as inflow hydrograph (or flow depth), inflow suspended sediment flux (or suspended sediment concentration), and inflow bed sediment flux (or bed sediment concentration) as

$$h(0,t) = h(t), \qquad t > 0.0, \tag{30}$$

$$c(0,t) = c(t) \qquad t > 0.0, \tag{31}$$

$$z(0,t) = z(t) \qquad t > 0.0. \tag{32}$$

[22] Equations (10)–(12) were solved using an explicit finite difference method. In order to overcome the problem of kinematic shocks, the method employed the Lax method [*Singh*, 1996]. Note that the finite difference equations were written for both the layers not only at the central nodes of the domain but also at the downstream node. All the

equations were solved simultaneously for each time step. The related finite difference equations are given as follows:

$$h_i^{j+1} = 0.5\left(h_{i+1}^j + h_{i-1}^j\right) - \frac{\Delta t\alpha\beta}{2\Delta x} h_{ij}^{\beta-1}\left(h_{i+1}^j - h_{i-1}^j\right) - \frac{p}{\left(1-c_i^j\right)}\left[z_i^{j+1} - 0.5\left(z_{i+1}^j + z_{i-1}^j\right)\right] + \frac{h_i^j}{\left(1-c_i^j\right)}\left[c_i^{j+1} - 0.5\left(c_{i+1}^j + c_{i-1}^j\right)\right] + \frac{\Delta t\alpha}{2\Delta x}\frac{h_{ij}^{\beta}}{\left(1-c_i^j\right)}\left(c_{i+1}^j - c_{i1}^j\right) + \frac{q_{lw}\Delta t}{\left(1-c_i^j\right)}, \quad (33)$$

$$c_i^{j+1} = 0.5\left(c_{i+1}^j + c_{i-1}^j\right) - \frac{\Delta t\alpha}{2\Delta x} h_{ij}^{\beta-1}\left(c_{i+1}^j - c_{i-1}^j\right) - \frac{c_i^j}{h_i^j}\left[h_i^{j+1} - 0.5\left(h_{i+1}^j + h_{i-1}^j\right)\right] - \frac{\Delta t\alpha\beta}{2\Delta x} c_i^j h_{ij}^{\beta-2}\left(h_{i+1}^j - h_{i-1}^j\right) + \frac{q_{lsus}\Delta t}{h_i^j} + \frac{\Delta t}{\rho_s h_i^j}\left[E_z^{ij} - D_c^{ij}\right], \quad (34)$$

$$z_i^{j+1} = 0.5\left(z_{i+1}^j + z_{i-1}^j\right) - \frac{\Delta t v_s}{2\Delta x}\left(1 - \frac{2z_i^j}{z_{\max}}\right)\left(z_{i+1}^j - z_{i-1}^j\right) + \frac{q_{ls}\Delta t}{(1-p)} + \frac{\Delta t}{(1-p)\rho_s}\left[D_c^{ij} - E_z^{ij}\right], \quad (35)$$

where i stands for space node and j stands for time node. Values Δt and Δx are time and space increments, respectively. Note that in equations (33)–(35), the unknowns are the variables at time node $(j + 1)$ (future time). Variables at time node j (the present time) are already known. For the numerical scheme, the stability conditions are found to be as

$$\frac{v_s\Delta t}{2\Delta x} \le 6 \times 10^{-6}, \quad (36)$$

$$\frac{\alpha\beta\Delta t}{2\Delta x} \le 1.2 \times 10^{-5}, \quad (37)$$

3. Model Application

[23] *Tayfur and Singh* [2006] simulated transient bed profiles in alluvial channels under equilibrium conditions using the kinematic wave theory. They tested their model using bead (glass sphere) experimental data of *Langbein and Leopold* [1968] and flume experimental data of *Soni* [1981a]. They also tested the performance of their model against that of the diffusion wave model. They have shown that the kinematic wave theory-based model can satisfactorily simulate transient bed profiles under equilibrium conditions. They also tested their model for hypothetical cases. Hypothetical cases involved investigating transient bed profiles under temporally varying flow and sediment inflows. They have shown the effects of different inflows on transient bed profiles along a channel length. In addition, they have shown the effects of sediment particle velocity (v_s) and maximum bed elevation ($z_{\max}$) on the movement of transient bed profiles. They have concluded that the model-simulated bed profiles seem theoretically reasonable for hypothetical cases and $z_{\max}$ and versus have a strong effect on transient bed profiles. Since *Tayfur and Singh* [2006] have already carried out hypothetical scenarios to test the components of the kinematic wave model, this study would be confined to testing the developed model against only experimental data obtained under nonequilibrium conditions.

4. Experimental Data

[24] The kinematic wave model was tested against the experimental data of aggradation and degradation depths measured by *Yen et al.* [1992] in laboratory flume experiments. *Yen et al.* [1992] used 72.0 m long and 1.0 m wide flume that had a bed slope of 0.0035. The water discharge was constant at a rate of 0.12 m^3/s. Sediment used in the experiment had a median diameter of 1.8 mm. At the beginning of the experiment, a sediment supply rate of 3.3 kg/min (dry mass) was continuously released from the upstream end until the channel bed reached a steady state of equilibrium. The sediment supply rate was then increased to 9.9 kg/min until a new equilibrium was reached. The rate of sediment supply was then reduced back to and kept at 3.3 kg/min until another new equilibrium was reached. Finally, the sediment supply was cut off, and only clear water was released from the upstream end until the channel bed was fully armored. Each period lasted for about 30 hours. Bed elevations were measured by bed-level gauges at six different locations during the experiments. The locations were 5 m apart from each other. A sluice gate at the downstream end of the flume was employed to maintain a constant tailwater level. The details of the experiment can be obtained from *Yen et al.* [1992].

[25] In model simulations, $z_{\max} = 0.10$ m was employed, since the water level was around 0.15 m. This value is also in agreement with *Langbein and Leopold* [1968]. The bed sediment porosity was assumed to be $p = 0.40$. This is in agreement with *Ching and Cheng* [1964]. Note that sediment was fed from the upstream end as a bed load and therefore at the upstream end suspended sediment concentration was zero.Figures 2a–2d show, respectively, simulations of bed profiles measured at 30, 60, 90, and 120 hours during the experimental run. The model satisfactorily simulated the measured data at 30, 60, 90, and 120 hours. The model closely predicted the measured data at each location along the bed, thus satisfactorily capturing the transient bed profiles at each simulation time. At the 60 hour simulation time, the model slightly underestimated the measured data at the end of the bed profile (Figure 2b). Figure 3 shows a scatter diagram comparing model predictions with measured data of Figure 2. As seen, predictions are satisfactory with a correlation coefficient of $R^2 = 0.98$. Figure 3 also shows a bandwidth with $\mp$2SE (where SE is the standard error) about the regression line, where the computed *SE* is 0.53 cm. As seen in Figure 3, there is only one point out of 24 points outside the bandwidth. In other words, bandwidth accounts for almost 96% of the scatter points. This implies that the developed numerical model can predict almost 96% of the measured data with $\mp$1.05 cm. The computed values of

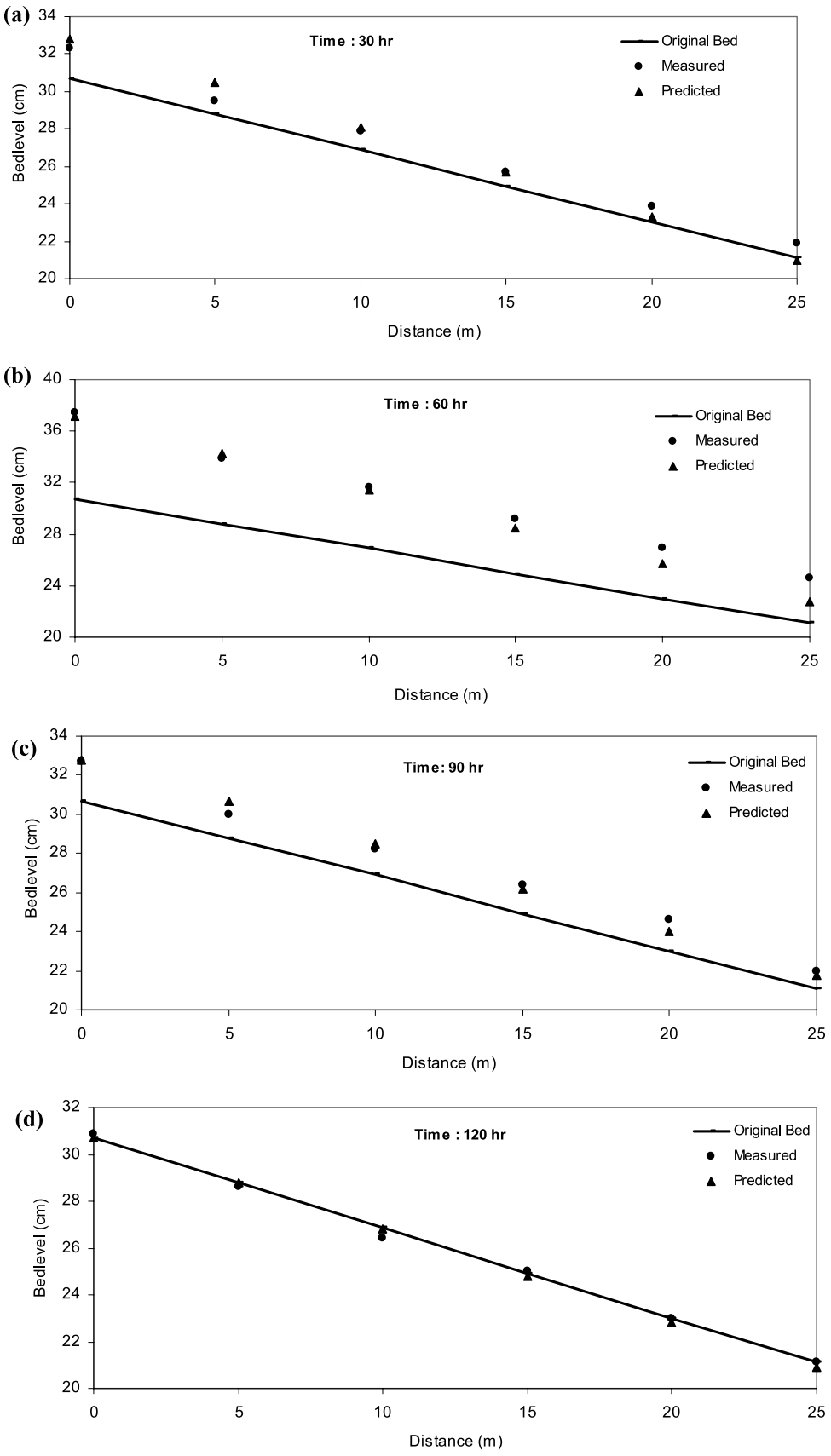

Figure 2. Simulation of bed profiles along a channel bed at (a) 30 h, (b) 60 h, (c) 90 h, and (d) 120 h of the laboratory experiment.

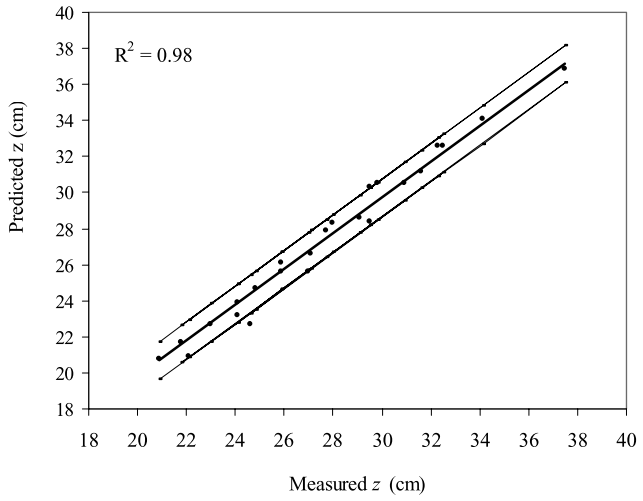

Figure 3. Measured bed elevations versus predicted bed elevations.

RMSE (root mean square error) and *MRE* (mean relative error) for Figure 3 are 0.70 cm, and 0.020, respectively. The mean relative error of *MRE* = 0.020 implies that the developed model makes about 2% error in predictions. These results imply a satisfactory performance of the newly developed model for predicting transient bed profiles along a channel bed.

[26] Figures 4a–4f present, respectively, simulations of bed levels measured at six different locations along the bed during the experimental period of 120 hours. Note that for the first 30 hours the sediment rate was supplied at a rate of 3.3 kg/min from the upstream end. Between 30 and 60 hours, the rate was 9.9 kg/min. Between 60 and 90 hours the rate was again kept at 3.3 kg/min, and after 90 hours the sediment rate was zero (clear water). Location 1 is 9.5 m away from the upstream end where the sediment supply was located. Locations 2, 3, 4, 5, and 6 are 5, 10, 15, 20, and 25 m away from location 1, respectively [*Yen et al.*, 1992]. The model simulations of transient bed levels at the specified locations are satisfactory. The model closely predicted

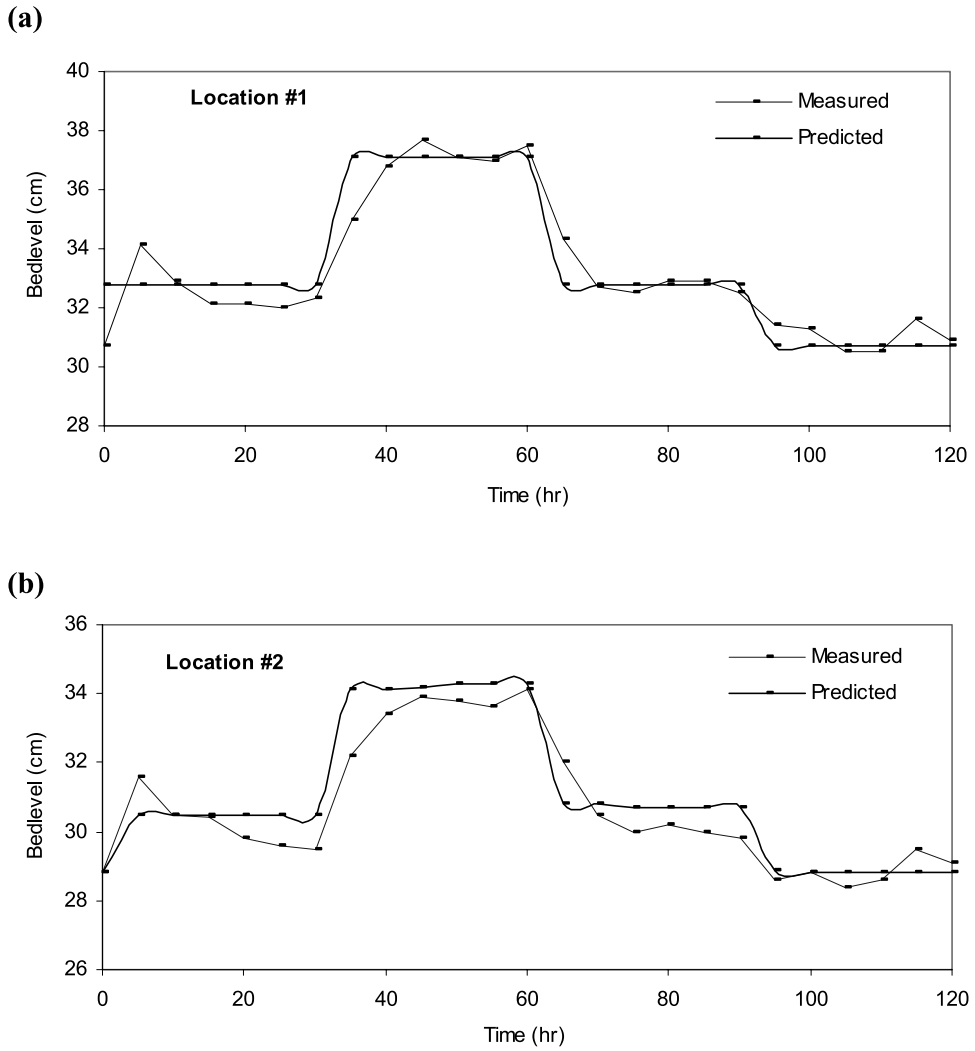

Figure 4. (a–f) Simulation of bed profiles in time during the laboratory experiment at six different locations of the experimental channel. Location 1 is 9.5 m away from the upstream end, where the sediment supplier was located. Locations 2, 3, 4, 5, and 6 are 5, 10, 15, 20, and 25 m away from location 1, respectively [*Yen et al.*, 1992].

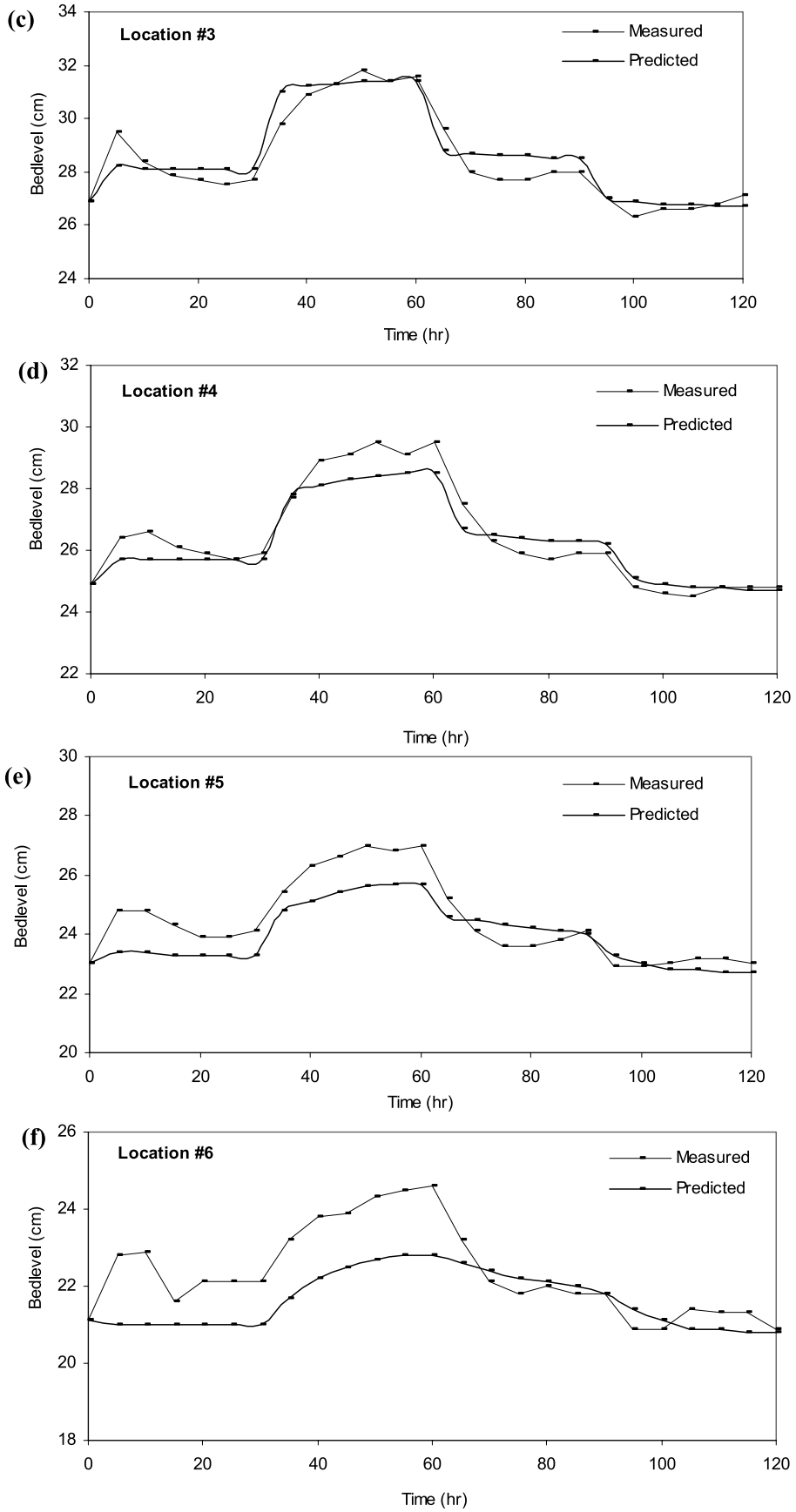

Figure 4. (continued)

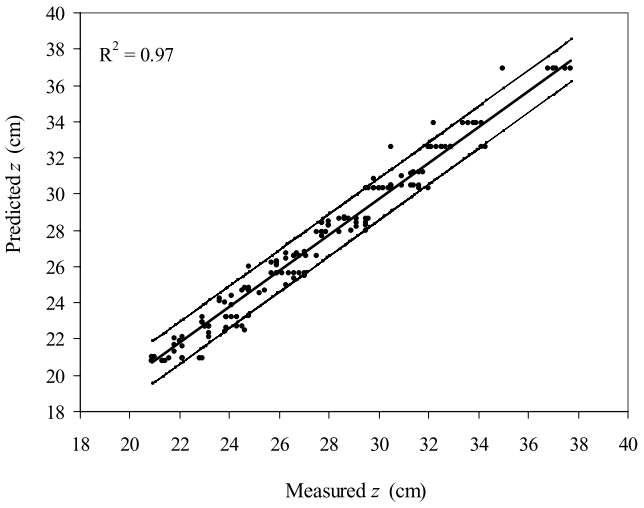

Figure 5. Measured bed elevations versus predicted bed elevations.

bed levels during rising, equilibrium, and recession periods satisfactorily, especially at locations 1, 2, 3, 4, and 5 (Figures 4a–4e). Although the model closely predicted measured data after 65 hours of the simulation time, it had a poor performance in predicting the measured data during the first 60 hours of the simulation time at location 6 (Figure 4f). It underestimated the measured data in the first 60 hours of the simulation time. Figure 5 shows the scatter diagram comparing model predictions with measured data of Figure 4. As seen, the predictions are satisfactory with a correlation coefficient of $R^2 = 0.97$. Figure 5 also shows a bandwidth with $\mp$2SE about the regression line, where the computed *SE* is 0.58 cm. As seen in Figure 5, there are 11 out of 150 points outside the bandwidth. In other words, bandwidth accounts for almost 93% of the scatter points. This implies that the developed numerical model can predict almost 93% of the measured data with $\mp$1.16 cm. The computed values of *RMSE* and *MRE* for Figure 5 are 0.79 cm, and 0.022, respectively. The mean relative error of *MRE* = 0.022 implies that the developed model makes about 2.2% error in the predictions. These results imply that the model, in general, performed well in predicting bed levels in time at each location satisfactorily.

5. Concluding Remarks

[27] This study developed the kinematic wave equations for simulating transient bed profiles in alluvial channels under nonequilibrium conditions. The model used a shear-stress approach to formulate flow transport capacity. The kinematic wave theory model employs a functional relation between sediment flux and sediment concentration and a relation between flow velocity and flow depth. The satisfactory simulation of transient bed profiles under nonequilibrium conditions in flume experiments implies that the developed model is plausible.

[28] It should be noted that the experiments against which the model was tested had nonequilibrium sediment transport due to the nonconstant sediment inflow at the upstream end of the flume. The flow discharge was, on the other hand, kept constant during the experiments, resulting in a steady and uniform flow. Therefore it would be beneficial to test the developed model against nonequilibrium sediment transport in nonuniform and unsteady flow, especially for such transport processes in the field.

Notation

c = volumetric sediment concentration in the water flow phase (in suspension) (L^3/L^3).
c_o = initial suspended sediment concentration (L^3/L^3).
c_{eq} = equilibrium suspended sediment concentration (L^3/L^3).
C_b = areal sediment concentration (M/L^2).
$C_{b\max}$ = maximum areal sediment concentration when transport ceases (M/L^2).
C_z = Chezy roughness coefficient ($L^{0.5}/T$).
D_c = the deposition rate ($M/L^2/T$).
d_s = particle diameter (L).
E_z = entrainment rate (detachment rate) ($M/L^2/T$).
g = gravitational acceleration (L/T^2).
h = flow depth (L).
h_o = initial (base) flow depth (L).
k = an exponent.
q_{lbed} = the lateral bed load sediment (L/T).
q_{ls} = lateral sediment flux (L/T).
q_{lw} = lateral water flux (L/T).
q_{lsus} = the lateral suspended sediment (L/T).
q_{sb} = sediment flux in the movable bed layer (L^2/T).
q_{ss} = unit suspended sediment discharge (M/L/T).
q_{st} = sediment transport rate ($M/L/T$).
Q_b = base flow rate.
Qeq = equilibrium flow rate.
p = porosity of sediment in the movable bed layer (L^3/L^3).
R^* = shear velocity Reynolds number.
R_{pn} = particle Reynolds number.
S_f = friction slope.
S_o = bed slope.
t = independent variable of time (T).
T_c = the flow transport capacity (M/L/T).
u = flow velocity (L/T).
u_c = critical flow velocity at the incipient sediment motion (L/T).
u^* = shear velocity (L/T).
v_f = the sediment particle fall velocity (L/T).
v_s = velocity of sediment particles as concentration approaches zero (L/T).
V_x = sediment mixing coefficient.
x = independent variable representing the coordinate in flow direction (L).
z = mobile bed layer elevation (L).
z_o = initial mobile bed layer elevation (L).
$z_{\max}$ = maximum bed elevation (L).
α = depth-velocity coefficient ($L^{0.5}/T$).
β = exponent.
δ = a constant.
λ = adaptation length.
$\prod$ = soil erodibility coefficient.
γ_s = specific weight of sediment (M/L^3).
γ_w = specific weight of water (M/L^3).
η = a coefficient.
ρ_s = sediment mass density (M/L^3).
σ = transfer rate coefficient (1/L).

τ = shear stress (M/L^2).
τ_c = critical shear stress (M/L^2).

References

Bridge, J. S., and S. J. Bennett (1992), A model for the entrainment and transport of sediment grains of mixed sizes, shapes, and densities, *Water Resour. Res.*, *28*(2), 337–363.

Bridge, J. S., and D. F. Dominic (1984), Bed load grain velocities and sediment transport rates, *Water Resour. Res.*, *20*(4), 476–490.

Cao, Z., and P. A. Carling (2003), On evolution of bed material waves in alluvial rivers, *Earth Surf. Processes Landforms*, *28*, 437–441.

Ching, H. H., and C. P. Cheng (1964), Study of river bed degradation and aggradation by the method of characteristics (in Chinese), *J. Hydraul. Eng.*, *5*, 41 pp.

Curran, J. C., and P. R. Wilcock (2005), Effect of sand supply on transport rates in a gravel-bed channel, *J. Hydraul. Eng.*, *131*(11), 961–967.

de Vries, M. (1965), Consideration about non-steady bed-load transport in open channels, paper 3.8 presented at XI Congress, Int. Assoc. of Hydraul. Res., Leningrad, Russia.

de Vries, M. (1973), River bed variation: Aggradation and degradation, *Pub. 107*, Delft Hydraul. Lab., Delft, Netherlands.

de Vries, M. (1975), A morphological time-scale for rivers, paper presented at XVI Congress, Int. Assoc. of Hydraul. Res., Sao Paulo, Brazil.

Dietrich, W. E. (1982), Settling velocity of natural particles, *Water Resour. Res.*, *18*(6), 1615–1626.

Foster, G. R. (1982), Modelling the erosion process, in *Hydrologic Modelling of Small Watersheds*, edited by C. T. Haan, H. P. Johnson, and D. L. Brakensiek, pp. 295–380, Am. Soc. of Agric. Eng., St. Joseph, Mich.

Gessler, J. (1965), The beginning of bedload movement of mixtures investigated as natural armouring in channels, W. M. Keck Lab. of Hydraul. and Water Resour., Calif. Inst. of Technol., Pasadena, Calif.

Hotchkiss, R. H., and G. Parker (1991), Shock fitting of aggradational profiles due to backwater, *J. Hydraul. Eng.*, *117*(9), 1129–1144.

Langbein, W. B., and L. B. Leopold (1968), River channel bars and dunes: Theory of kinematic waves, *U. S. Geol. Surv. Prof. Pap.*, *422-L*, 20 pp.

Li, S. S., and R. G. Millar (2007), Simulating bed-load transport in a complex gravel-bed river, *J. Hydraul. Eng.*, *133*(3), 323–328.

Lisle, T. E., Y. T. Cui, G. Parker, J. E. Pizzuto, and A. M. Dodd (2001), The dominance of dispersion in the evolution of bed material waves in gravel-bed rivers, *Earth Surf. Processes Landforms*, *26*, 1409–1420.

Lyn, D. A., and M. Altinakar (2002), St. Venant-Exner equations for near-critical and transcritical flows, *J. Hydraul. Eng.*, *128*(6), 579–587.

Mahmood, K. (1975), Mathematical modeling of morphological transients in sandbed canals, paper BB presented at XVI Congress, Int. Assoc. of Hydraul. Res., Sao Paulo, Brazil.

Mohammadian, A., M. Tajrishi, and F. L. Azad (2004), Two-dimensional numerical simulation of flow and geo-morphological processes near headlands by using unstructured grid, *Int. J. Sediment. Res.*, *19*(4), 258–277.

Phillips, B. C., and A. J. Sutherland (1983c), Mathematical modeling of lag effects in bed load transport, paper presented at 8th Australian Fluid Mechanics Conference, Univ. of Newcastle N.S.W., Australia, 28 Nov. to 2 Dec.

Pianese, D. (1994), Comparison of different mathematical models for river dynamics analysis, paper 782 presented at International Workshop on Floods and Inundations Related to Large Earth Movements, Int. Assoc. of Hyraul. Eng. and Res., Trento, Italy, 4–7 Oct.

Ribberink, J. S., and J. T. M. Van Der Sande (1985), Aggradation in rivers due to overloading: Analytical approaches, *J. Hydraul. Res.*, *23*(3), 273–283.

Singh, A. K., U. C. Kothyari, and K. G. R. Raju (2004), Rapidly varying transient flows in alluvial rivers, *J. Hydraul. Res.*, *42*(5), 473–486.

Singh, V. P. (1996), *Kinematic Wave Modeling in Water Resources: Surface Water Hydrology*, John Wiley, New York.

Soni, J. P. (1981a), Laboratory study of aggradation in alluvial channels, *J. Hydrol.*, *49*, 87–106.

Soni, J. P. (1981b), An error function solution of sediment transport in aggradation channels, *J. Hydrol.*, *49*, 107–119.

Soni, J. P. (1981c), Unsteady sediment transport law and prediction of aggradation parameters, *Water Resour. Res.*, *17*(1), 33–40.

Tang, X., and D. W. Knight (2006), Sediment transport in river models with overbank flows, *J. Hydraul. Eng.*, *132*(1), 77–86.

Tayfur, G. (2002), Applicability of sediment transport capacity models for non-steady state erosion from steep slopes, *J. Hydrol. Eng.*, *7*(3), 252–259.

Tayfur, G., and V. P. Singh (2006), Kinematic wave model of bed profiles in alluvial channels, *Water Resour. Res.*, *42*, W06414, doi:10.1029/2005WR004089.

Vreugdenhil, C. B., and de M. Vries (1973), Analytical approaches to non-steady bedload transport, *Res. Rep. S 78*, part IV, 16 pp., Delft Hydraul. Lab., Delft, Netherlands.

Wilcock, P. R., and J. C. Crowe (2003), Surface-based transport model for mixed-size sediment, *J. Hydraul. Eng.*, *129*(2), 120–128.

Wilcock, P. R., S. T. Kenworthy, and J. C. Crowe (2001), Experimental study of the transport of mixed sand and gravel, *Water Resour. Res.*, *37*(12), 3349–3358.

Yang, C. T. (1996), *Sediment Transport Theory and Practice*, McGraw-Hill, New York.

Yen, C. L., S. Y. Chang, and H. Y. Lee (1992), Aggradation-degradation process in alluvial channels, *J. Hydraul. Eng.*, *118*(12), 1651–1669.

V. P. Singh, Department of Biological and Agricultural Engineering, Texas A&M University, Scoates Hall, 2117 TAMU, College Station, TX 77843-2117, USA. (vsingh@tamu.edu)

G. Tayfur, Department of Civil Engineering, Izmir Institute of Technology, Urla, Izmir 35340, Turkey. (gokmentayfur@iyte.edu.tr)